Available online at www.sciencedirect.com
ScienceDirect
Journal of Crystal Growth 303 (2007) 253–257
JOURNAL OF CRYSTAL GROWTH
www.elsevier.com/locate/jcrysgro

Numerical modeling of melt flows in vertical Bridgman configuration affected by a rotating heat field

K.A. Kokh[a,*], V.N. Popov[b], A.E. Kokh[a], B.A. Krasin[c], A.I. Nepomnyaschikh[c]

[a]Institute of Geology and Mineralogy SB RAS, Novosibirsk, Russia
[b]Institute of Theoretical and Applied Mechanics SB RAS, Novosibirsk, Russia
[c]Institute of Geochemistry SB RAS, Irkutsk, Russia

Available online 16 January 2007

Abstract

In this work, the numerical modeling of convection in a vertical Bridgman system under the influence of a rotating heat field was studied. First results show that changing of the heating from an axi-symmetric to a non-symmetric non-stationary configuration results in an increase in the convective flow and thus led to an increase of the melt uniformity because the convective cell is occupying almost the entire melt domain. Experimental growth of polycrystalline silicon under such special conditions provided ingots with improved texture and uniformity of electronic properties.

PACS: 81.10.-h; 07.05.Tp; 47.32.Ef; 84.60.Jt

Keywords: A1. Computer simulation; A1. Convection; A1. Heat field symmetry and rotation; A2. Bridgman technique; B1. Polycrystalline silicon; B3. Solar cells

1. Introduction

The Bridgman technique is one of the most important methods for the growth of various materials. An important issue of this methods is the development of new approaches to influence convection. This work is devoted to the numerical simulation of a new method of a rotating heat field applied to Bridgman technique being developed in the Crystal Growth Lab of IGM SB RAS.

The idea of implementation of the method consists in the change of the vertical temperature profile to a "destabilized" configuration at one side of the container within the melt with maintenance of a "stabilized" one at the other side (Fig. 1a). In this case, a strong convective role is expected to occupy the entire melt domain, which is contrary to the case with axi-symmetric stabilized configuration, where only weak convection exists (Fig. 1b). Further rotation of the cell around vertical axis of the container is likely to produce a more uniform melt by stirring. This may be achieved by two ways: (a) rotation of the container in the above described non-axi-symmetric heat field, and (b) rotation of the heat field around a fixed container, e.g. by means of commutation of heating elements [1].

However, the two variants are not fully equivalent. In the case of a container rotation, additional Coriolis force takes place. On the other hand, the contribution of this force seems to be small since the container rotation should be slow enough in order to transfer the non-axi-symmetric heat field to the distribution of the temperature in the melt. Also there is a smooth translation of the overheated sector in the first approach due to rotation of the container in non-axi-symmetric heat field. This work is devoted to the modeling of the second approach that presumes a discrete (stepwise) translation of the sector due to a stepwise switching of the vertically aligned heating elements. On the other hand, we consider the heat transfer from 12 heaters that seems to provide enough smooth translation. Hence, we consider that the calculated results show principally the behavior of the melt for any of these approaches.

*Corresponding author. Tel./fax: +7 383 3333947.
E-mail address: k.a.kokh@gmail.com (K.A. Kokh).

0022-0248/$ - see front matter © 2006 Elsevier B.V. All rights reserved.
doi:10.1016/j.jcrysgro.2006.11.153

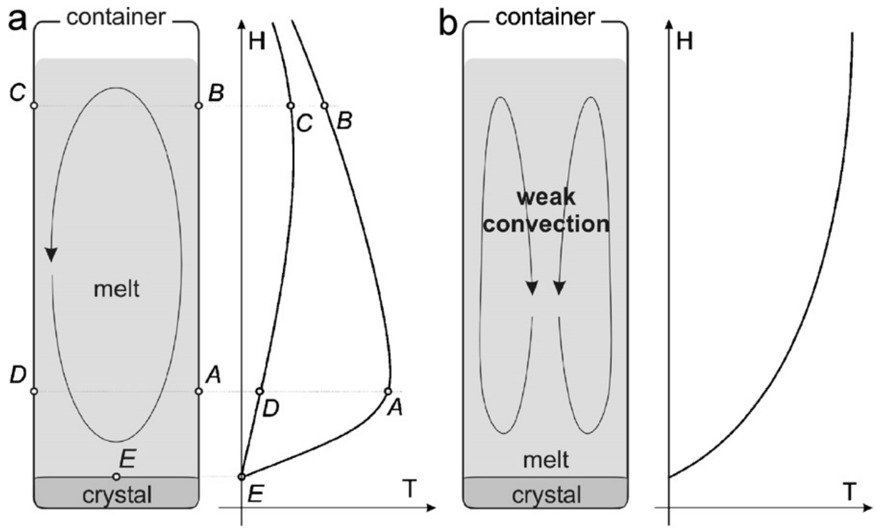

Fig. 1. Non-axi-symmetric (a) and standard axi-symmetric (b) axial temperature distributions applied to vertical Bridgman system.

At the end of this paper, first results of experiments of polycrystalline silicon grown in a rotating heat field using the second approach are given.

2. Model description

Fig. 2 shows a sketch of the model. A container of radius R_0 is filled with a melt of height H_0. The temperature distribution at the side walls is defined by 12 vertical heaters around the container. The temperature T_0 of the overheated sector $(H_0-Z_0)R_0\Delta\varphi$ contributes to the temperature T_H above Z_0 produced by other heaters. The temperature at the bottom is correlated with the phase transition temperature T_S. The mathematical description of the problem using Navier–Stokes and heat-transfer equations is as follows:

$$\mathbf{u}_t + (\nabla \cdot \mathbf{u})\mathbf{u} = -\nabla P + \nabla^2 \mathbf{u} + \mathbf{k} Gr\theta, \quad \nabla \cdot \mathbf{u} = 0,$$

$$\theta_t + (\nabla \cdot \mathbf{u})\theta = \frac{1}{Pr}\nabla^2\theta, \quad \theta = (T - T_S)/(T_0 - T_S).$$

Here $\mathbf{u}$ is the velocity vector with u, v and w components in radial, azimuthal and vertical directions, respectively; $\mathbf{k}$ is the unit vector along the coordinate axis z, P the pressure; θ the temperature, Pr the Prandtl number, Gr the Grashoff number, Bi the Biot number, where $Pr = v/a$, $Gr = \beta g R_0^3 \Delta T_0/v^2$, $Bi = \alpha R_0/\lambda$.

The dimensionless values are determined through following characteristic parameters: R_0—dimensional radius of the container; $t_0 = R_0^2/v$,—time; $v_0 = v/R_0$—velocity; $P_0 = v^2\rho/R_0^2$—pressure; $\Delta T_0 = T_H - T_S$—temperature interval; where: T_S is the melting point, v the kinematic viscosity; ρ the density, g the gravitational acceleration, β the thermal volume expansion coefficient, λ the thermal conductivity, a the temperature conductivity, and α the heat dissipation coefficient.

No-slip condition was imposed to the walls of the container. Also we assume that convection is not strong to produce viscous tensions on the surface providing a flat boundary. Newton's law describes the heat transfer out of the melt container. The temperature at the phase boundary is supposed to be constant. Initial condition is that the whole melt is heated up to T_H except the region near the flat crystallization front.

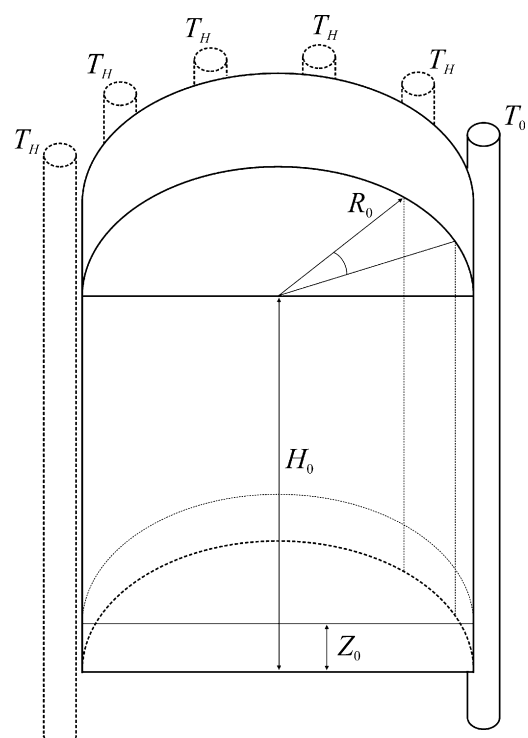

Fig. 2. Sketch of the model.

Boundary conditions:

at the bottom of the container

$$\mathbf{u} = 0, \quad \theta = 0, \quad 0 \leqslant r \leqslant R_0, \quad z = 0, \quad 0 \leqslant \varphi \leqslant 2\pi;$$

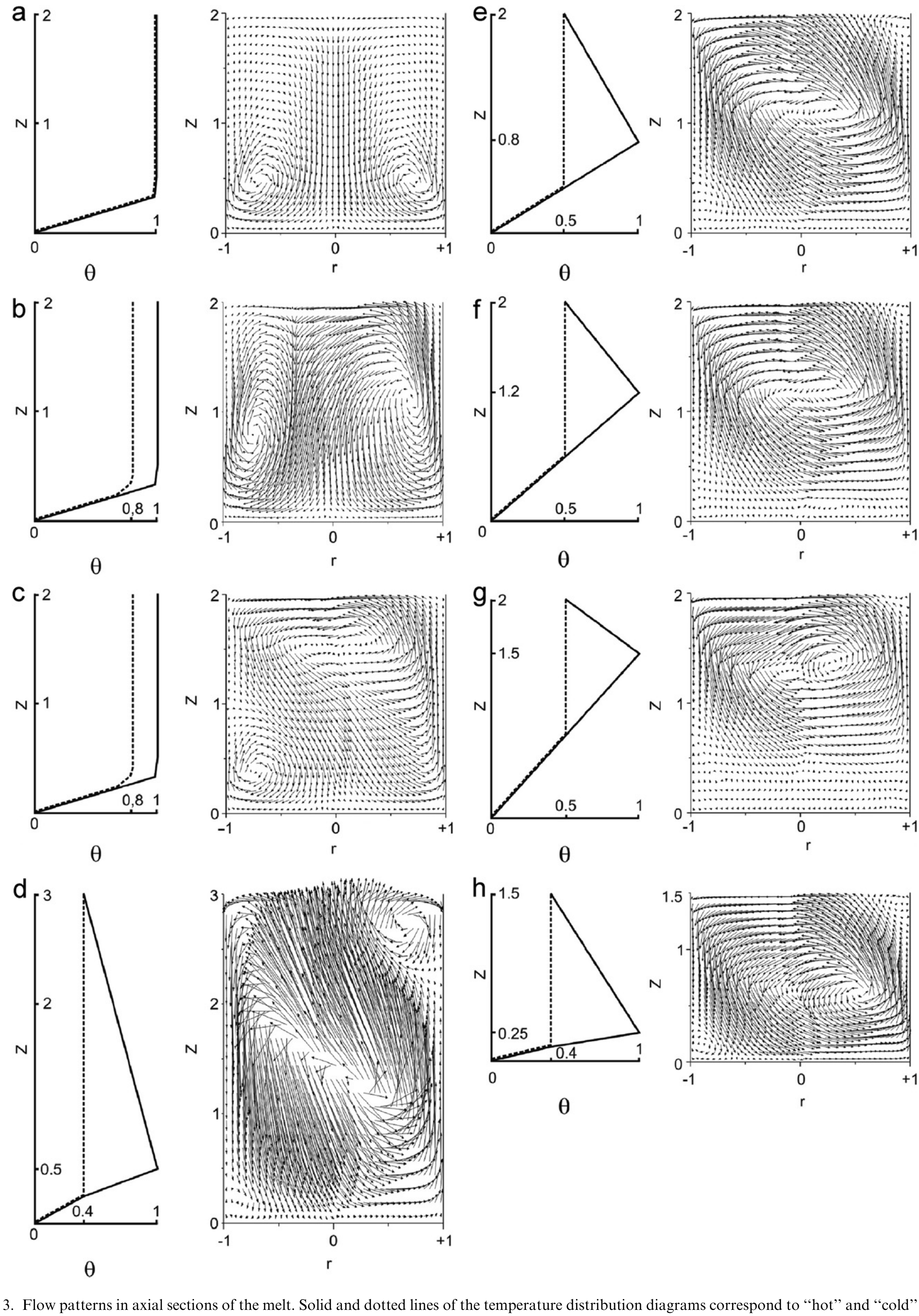

Fig. 3. Flow patterns in axial sections of the melt. Solid and dotted lines of the temperature distribution diagrams correspond to "hot" and "cold" sides of the container.

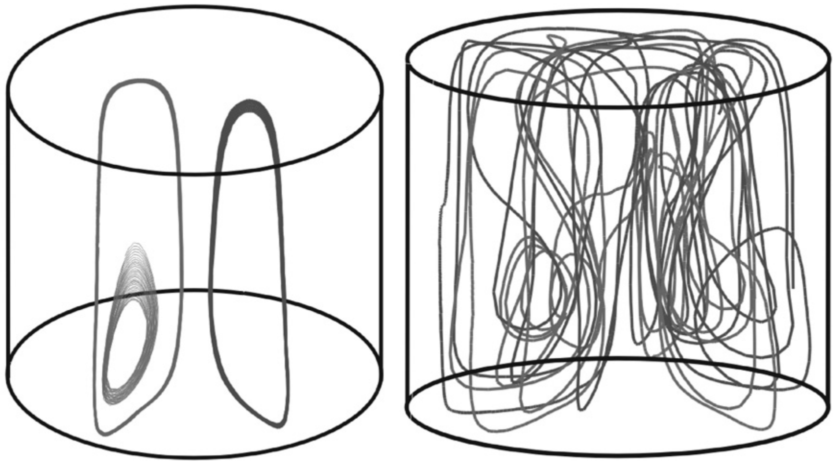

Fig. 4. Calculated marker trajectories for axi-symmetric (a) and non-axi-symmetric non stationary (b) heating.

at the side walls of the container ($r = 1,\ 0 \leqslant \varphi \leqslant 2\pi$) $\mathbf{u} = 0$; $0 < z \leqslant H_0; \frac{\partial \theta}{\partial r} = Bi_1 \theta_H z/Z_0,\ 0 \leqslant z \leqslant Z_0$,

$$\frac{\partial \theta}{\partial r} = \begin{cases} Bi_1[\theta_0(z) - \theta], & \varphi \in \Delta, \\ Bi_1[\theta_H - \theta], & \varphi \notin \Delta, \end{cases}$$

$Z_0 < z \leqslant H_0, \Delta$—overheated zone, $\theta_0(z)$—temperature distribution along ''overheated'' wall;

at the surface of the melt

$$\frac{\partial u}{\partial z} = 0, \quad \frac{\partial v}{\partial z} = 0, \quad w = 0, \quad \frac{\partial \theta}{\partial z} = -Bi_2\theta, \quad 0 \leqslant r < 1,$$
$$z = H_0, \quad 0 \leqslant \varphi \leqslant 2\pi.$$

Initial conditions ($t = 0$): $\mathbf{u} = 0,\ 0 \leqslant r \leqslant 1,\ 0 \leqslant z \leqslant H_0,\ 0 \leqslant \varphi \leqslant 2\pi;\ \theta = \theta_H \cdot z/Z_0,\ 0 \leqslant z \leqslant Z_0,\ \theta = \theta_H,\ Z_0 < z \leqslant H_0,\ 0 \leqslant r \leqslant 1,\ 0 \leqslant \varphi \leqslant 2\pi$.

3. Results of simulations

In this work, we present some numerical results that illustrate possible flow patterns in the melt heated by 12 switchable vertical heating elements. A sector $\pi R_0/6$ ($\Delta\varphi = \pi/6$) of the container wall is heated by one element. We study the flow patterns in a silicon melt as a model liquid. The dimensionless parameters used for the calculations are: $Pr = 0.0127$, $Gr = 10^6$, $Bi_1 = 50$, $Bi_2 = 0.05$. The calculations were performed on $30 \times 36 \times 40$ grid in radial, azimuthal and vertical directions, correspondingly. The time step of 10^{-4} was chosen to achieve stability of the numerical calculations and convergence of the iterations. We studied stationary and non-stationary heat fields. In the last case, a time interval between the stepwise switching of the heating elements equal to 0.2 was considered.

Fig. 3 shows flow patterns in axial section of the container for different configurations of a stationary heat field. The flow pattern produced by the uniform axi-symmetric heat field is shown at Fig. 3a. In that case, slow convection forming a toroidal cell is observed in the lower half of the melt domain. Additional heating of the wall in the $\Delta\varphi = 30^\circ$ segment results in a change of the melt flow (Fig. 3b). The cell becomes non-axi-symmetric forming more intensive flow along the ''overheated'' wall. Increasing of the segment by additional heating at 90° causes further expansion of the developing vortex to the upper parts of the melt domain (Fig. 3c). Practically, this corresponds to the heating from three joint elements.

Fig. 3d shows the flow pattern in the case of a ''destabilized'' temperature distribution along one side of the container. The flow in the dominant vortex becomes more intensive, likely to provide better mixing in the melt. Besides the main vortex, two minor vortices in opposite corners of the melt domain are observed. Figs. 3e–g illustrate convection depending on the vertical position of the maximum of the temperature distribution. One may see that the dominant vortex follows the maximum, which agrees with the results of numerical simulations of a ''local heating source'' performed in Ref. [2]. Another result of our computation is shown at Figs. 3d,e,h. It was found, that the cell occupying almost the entire melt domain exists in spite of a change of the melt height. Thus, it is possible to provide stable mixing in the melt during the whole process of crystal growth.

A better illustration of the mixing is shown by marker trajectories in Fig. 4. Stationary axi-symmetric heating provides a stable and closed trajectory in one plane (Fig. 4a). While revolving of the hot zone around the container (heat field rotation) produces a three-dimensional movement that passes through the whole melt domain (Fig. 4b).

4. Growth of polycrystalline silicon in a non-symmetric heat field

As it was mentioned in the introduction, that a rotation of the heat field may be realized in two variants. Experiments using the second approach were performed in Ref. [1]. In this work, we studied the growth of photovoltaic polycrystalline silicon by the Bridgman technique using a first approach—rotation of the container in the stationary non-axi-symmetric heat field.

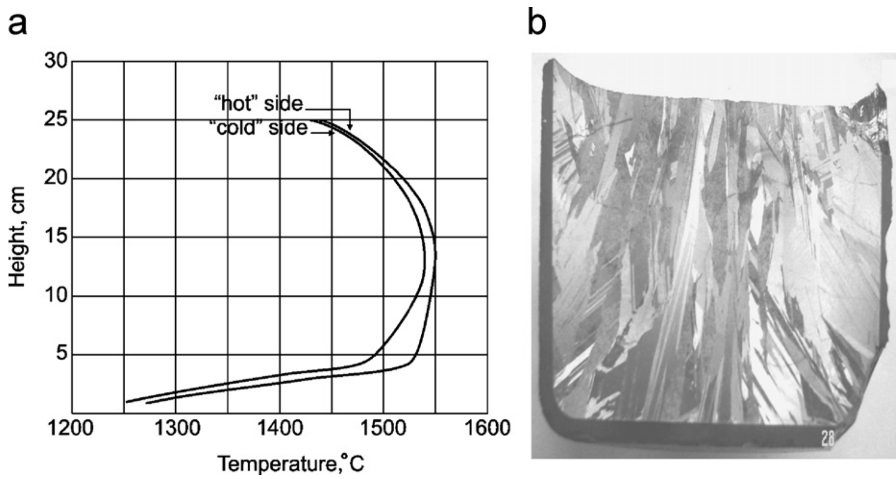

Fig. 5. Non-axi-symmetric temperature distributions along the graphite heater (a) and axial section of polycrystalline silicon ingot grown in rotating heat field (b).

The matter of investigation relates to the improvement of the efficiency of polycrystalline silicon in solar cells. This may be achieved by an improvement of the grain size, texture, orientation of the individual crystals and by a minimization of inclusions [3,4]. In the process technology, it is desirable to grow ingots with large-grain size and parallel orientation of columnar crystals. An important feature of the sectioned samples is the minimal length of the boundaries between grains, in the area of crystallites of several mm^2, with uniform distribution of electronic properties. Achievement of the goals depends both on purity of the starting material and definitely on the growth conditions.

The major part of our experiment concerned the redesigning of the graphite heater. So the conditions for crucible rotation in a stationary non-axi-symmetric heat field were created. The heat field is described by different axial temperature distributions along opposite walls (Fig. 5a). Conical crucibles from amorphous graphite 70 mm in height and 50–65 mm in diameter were used. We studied Bridgman crystallization of polycrystalline ingots from silicon of refined metallurgic and electronic grades. Experiments with crucible rotation and pulling rates in the range of 1–0.18 rpm and 2.5–1 $cm\,h^{-1}$, respectively, were performed.

Our experiments showed the possibility of a reproducible improvement of the structure and texture by using the following growth parameters: temperature gradient in growth zone 8.5 $K\,cm^{-1}$, crucible rotation 1.2 rpm, crucible transition 1.2 $cm\,h^{-1}$. These growth parameters result in ingots with large crystals growing from bottom to top of the container (Fig. 5b).

Analysis of the grains shows low dislocation density ($0.82 \times 10^5\,cm^{-2}$) and uniform distribution of electronic properties (specific resistance 1.8 $\Omega\,cm$, charge carrier mobility 252 $cm^2\,V^{-1}\,s^{-1}$, minority charge carrier lifetime 27 μs).

5. Conclusion

Three-dimensional numerical modeling was performed to investigate convective flows in a silicon melt under a rotating non-axi-symmetric heat field. The results show that changing of the heating from axi-symmetric to non-axi-symmetric non stationary configurations results both in intensifying of the convective flow and in increasing of the melt uniformity due to azimuthal components of the melt flow. The growth of polycrystalline silicon in a rotating heat field showed the possibility of a reproducible improvement of the material properties. Thus we demonstrated the possibility of control of the heat and mass transfer processes during crystal growth by means of a rotating heat field.

Acknowledgment

The work is supported by RFBR grant No. 05-05-64752.

References

[1] K.A. Kokh, B.G. Nenashev, A.E. Kokh, G.Yu. Shvedenkov, J. Crystal Growth 275 (2005) E1964.
[2] Yeckel, G. Compere, A. Pandy, J.J. Derby, J. Crystal Growth 263 (2004) 629.
[3] B.A. Krasin, A.I. Nepomnyaschikh, A.S. Tokarev, T.S. Shamirzaev, R.V. Presnyakov, A.P. Maxikov, Mater. Electron. Tech. 1 (2005) 28 (in Russian).
[4] K. Fujiwara, Y. Obinata, T. Ujihara, N. Usami, G. Sazaki, K. Nakajima, J. Crystal Growth 226 (2004) 441.